

Article

# Photoinduced Cu(II)-Mediated RDRP to P(VDF-*co*-CTFE)-*g*-PAN

Xin Hu <sup>1,4</sup> , Guopeng Cui <sup>2,4</sup>, Ning Zhu <sup>2,4</sup> , Jinglin Zhai <sup>2,4</sup> and Kai Guo <sup>2,3,4,\*</sup> 

<sup>1</sup> College of Materials Science and Engineering, Nanjing Tech University, Nanjing 211800, China; xinhu@njtech.edu.cn

<sup>2</sup> College of Biotechnology and Pharmaceutical Engineering, Nanjing Tech University, Nanjing 211800, China; 851032931@njtech.edu.cn (G.C.); ningzhu@njtech.edu.cn (N.Z.); 18852001050@njtech.edu.cn (J.Z.)

<sup>3</sup> State Key Laboratory of Materials-Oriented Chemical Engineering, Nanjing Tech University, Nanjing 211800, China

<sup>4</sup> Jiangsu National Synergetic Innovation Centre for Advance Materials, Nanjing Tech University, Nanjing 211800, China

\* Correspondence: guok@njtech.edu.cn; Tel.: +86-25-5813-9926

Received: 12 December 2017; Accepted: 10 January 2018; Published: 13 January 2018

**Abstract:** Photoinduced Cu(II)-mediated reversible deactivation radical polymerization (RDRP) was employed to synthesize poly(vinylidene fluoride-*co*-chlorotrifluoroethylene)-*graft*-polyacrylonitrile (P(VDF-*co*-CTFE)-*g*-PAN). The concentration of copper catalyst (CuCl<sub>2</sub>) loading was as low as 1/64 equivalent to chlorine atom in the presence of Me<sub>6</sub>-Tren under UV irradiation. The light-responsive nature of graft polymerization was confirmed by “off-on” impulsive irradiation experiments. Temporal control of the polymerization process and varied graft contents were achieved via this photoinduced Cu(II)-mediated RDRP.

**Keywords:** fluoropolymer; photoinduced; copper-mediated RDRP; graft; PAN

## 1. Introduction

Atom transfer radical polymerization (ATRP) [1–4] has been one of the most powerful reversible deactivation radical polymerization (RDRP) methodologies for the synthesis of well-defined polymers [5–8]. The original ATRP was conducted with a high concentration of Cu(I) catalyst (equivalent to alkyl halide initiator) in order to compensate for unavoidable radical termination reactions. A series of ATRP variants have been developed to reduce the catalyst loading. Activators regenerated by electron transfer (ARGET) ATRP [9], initiators for continuous activator regeneration (ICAR) ATRP [10], electrochemically-mediated ATRP (eATRP) [11], and Cu(0)-mediated RDRP [12–15] have been proposed to decrease the copper concentration below 100 ppm.

Photopolymerization has become increasingly popular thanks to its unique advantages in temporal and spatial control [16–20]. Photoinduced Cu(II)-mediated RDRP achieved remarkable progress in tailor-made polymer synthesis [21–24]. The combination of low-concentration CuBr<sub>2</sub> and excess *tris*[2-(dimethylamino)ethyl]amine (Me<sub>6</sub>-Tren) exhibited outstanding efficiency in acrylate polymerizations [25,26]. Well-defined homopolymers, telechelic block copolymers, brush polymers, and sequence controlled polymers were obtained via photoinduced Cu(II)-mediated RDRP [27–35]. Iridium [36–39] and ruthenium [40] complexes were also found to be effective photocatalysts to mediate visible light-induced ATRP. Recently, organocatalyzed ATRP (OATRP) was established to generate metal-free polymers by using photoredox catalyst [41–51]. This young yet rapidly growing research area would attract broad interest from both academia and industry.

Poly(vinylidene fluoride-*co*-chlorotrifluoroethylene) (P(VDF-*co*-CTFE)) is one of the most used high-performance fluoropolymers with various applications [52]. Several kinds of chemical and

physical modification strategies have been presented to improve the functionality and compatibility of fluoropolymers. ATRP was also employed to synthesize P(VDF-*co*-CTFE)-*g*-polystyrene (PS) and P(VDF-*co*-CTFE)-*g*-polyacrylates [53–55]. The dielectric and energy storage properties were enhanced by the introduction of graft chains, which could reduce the remnant polarization of the fluoropolymer [54]. This Cu(I)-mediated process required relative high catalyst loading and elevated reaction temperature to initiate the less active C–Cl bond in P(VDF-*co*-CTFE) backbone, which resulted in unexpected chain transfer reactions and dehydrochlorination reactions [56]. Cu(0)-mediated RDRP of acrylonitrile (AN) and methyl methacrylate (MMA) in the presence of P(VDF-*co*-CTFE) allowed colorless and purer P(VDF-*co*-CTFE)-*g*-PAN and P(VDF-*co*-CTFE)-*g*-PMMA copolymers for its mild reaction conditions and lower catalyst concentration [57–59]. Improvements were achieved by transferring the polymerization from a batch reactor to a copper tubular reactor, such as diminished inconsistent induction time, suppressed “hot spot” effect, and decreased copper and ligand concentration [60].

Herein, photoinduced Cu(II)-mediated RDRP was utilized for the graft modification of P(VDF-*co*-CTFE) (Scheme 1). Polymerizations of acrylonitrile in the presence of CuCl<sub>2</sub>/Me<sub>6</sub>-Tren under UV irradiation was investigated to evaluate its effect on the preparation of P(VDF-*co*-CTFE)-*g*-PAN with low catalyst concentration and temporal control of the polymerization process.

## 2. Experimental Section

### 2.1. Materials

P(VDF-*co*-CTFE) was provided by Solvay Solex (Brussels, Belgium) (Dyneon 31008, with the [VDF]:[CTFE] = 94:6, containing 0.89 mmol chlorine atom per gram). Acrylonitrile (AN) (J&K, Beijing, China, 99%) was washed by 5 wt % aqueous sodium hydroxide solution three times, and was subsequently rinsed with deionized water until neutralization. The resultant solution was dried overnight with anhydrous MgSO<sub>4</sub>, then distilled under reduced pressure to remove extant inhibitor and stored under N<sub>2</sub> at –20 °C. Dimethyl sulfoxide (DMSO) (Xilong Chemical, Shenzhen, China, AR) was distilled under vacuum from CaH<sub>2</sub>. Other reagents were used as received. The source of the UV light (Shany Cosmetics Company, New York, NY, US) setup was a commercially available UV nail gel curing lamp with four 9 W bulbs (36 W, λ<sub>max</sub> ~365 nm, item model number: SH-KD-UVLAMP36W).

### 2.2. Synthesis Procedure

Polymerizations were conducted by using a Schlenk technique [57]. First, 0.500 g of P(VDF-*co*-CTFE) (VDF:CTFE = 94:6) (containing 0.445 mmol Cl atom) was dissolved in 10 mL DMSO with stirring before CuCl<sub>2</sub>·2H<sub>2</sub>O (2.4 mg, 0.0140 mmol) and Me<sub>6</sub>-Tren (19.2 mg, 0.0834 mmol) were added under N<sub>2</sub> atmosphere. After adding 0.88 mL AN (13.35 mmol), the reactant mixture ([Cl]:[Cu]:[Me<sub>6</sub>-Tren]:[AN] = 1:(1/32):(6/32):30) was put into the ultraviolet light (λ<sub>max</sub> ~365 nm) while cooling with a hair dryer. Samples were taken at regular time intervals followed by precipitation in H<sub>2</sub>O/CH<sub>3</sub>OH (*v*:*v* = 1:1) mixture, washed three times with ethyl alcohol, and dried overnight under reduced pressure. The resultant graft copolymer was obtained for characterization.

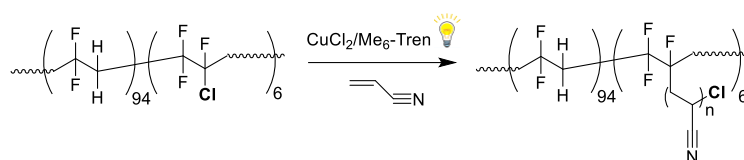
### 2.3. Characterization

Nuclear magnetic resonance (NMR) spectra were recorded on a Bruker (Rheinstetten, Germany) (Advance III) 400 MHz instrument for solutions in DMSO-*d*<sub>6</sub> containing tetramethylsilane (TMS) as internal standard. Fourier transform infrared (FTIR) spectroscopy of polymer films was performed on a Nicolet iS5 (Thermo Scientific, Madison, WI, US). Differential scanning calorimetric (DSC) analysis was conducted on a Discovery DSC 250 (TA instruments, New Castle, DE, US). After rapid heating and cooling cycles (at a rate of 20 °C/min) to remove the thermal history, the sample was heated at a rate of 10 °C/min under nitrogen atmosphere. Thermogravimetric analysis (TGA) (TA instruments,

New Castle, DE, US) results were recorded on Netzsch STA 449 F3 Jupiter (Selb, Germany) in nitrogen atmosphere at a heating rate of 10 °C/min.

### 3. Results and Discussion

Poly(acrylonitrile) (PAN) and its copolymers have been widely used as precursors for novel carbon materials with outstanding properties and performances [43]. P(VDF-*co*-CTFE)-*g*-PAN copolymers could be synthesized via Cu(0)-mediated reversible deactivation radical polymerization (RDRP) in batch and flow reactors [57,60]. Comparing with traditional ATRP protocol, copper catalyst loading was as low as about 1/4 equivalent to the chlorine atoms in the batch reactor. Copper catalyst, however, is highly desirable to decrease in order to reduce the amount of metal residue, which would potentially influence the application of final material. Inspired by the work about photoinduced Cu(II)-mediated RDRP [25,26], CuCl<sub>2</sub>/Me<sub>6</sub>-Tren was employed to promote the polymerizations of AN with P(VDF-*co*-CTFE) as macroinitiator. The polymerization results are listed in Table 1. After 6 h of UV irradiation ( $\lambda \sim 365$  nm, 36 W) while cooling with a hair dryer, P(VDF-*co*-CTFE)-*g*-PAN (graft content = 20.8 mol %) was obtained with a low copper concentration ([Cl]:[Cu]:[L]:[AN] = 1:(1/32):(6/32):30) (Table 1, run 5) according to NMR analysis [57]. A 13.4 mol % graft content was achieved, even upon reducing the catalyst feed ratio into 1/64 (Table 1, run 7). This would be favorable for the applications of resultant graft copolymers in dielectric devices.



**Scheme 1.** Photoinduced Cu(II)-mediated reversible deactivation radical polymerization (RDRP) to P(VDF-*co*-CTFE)-*g*-PAN. P(VDF-*co*-CTFE): poly(vinylidene fluoride-*co*-chlorotrifluoroethylene); PAN: poly(acrylonitrile).

**Table 1.** Summary of photoinduced Cu(II)-mediated RDRP of AN in DMSO with P(VDF-*co*-CTFE) as macroinitiator under UV ( $\lambda_{\max} = 365$  nm) irradiation for 6 h.

Run	[Cl]:[Cu]:[L]:[AN]	Conversion%	Graft content <sup>[a]</sup> mol %	Graft length <sup>[b]</sup>
1 <sup>[c]</sup>	1:(1/32):(6/32):30	0	0	0
2	0:(1/32):(6/32):30	0	-	-
3	1:(0):(0):30	0	0	0
4	1:(1/32):(4/32):30	10.0	17.2	2.9
5	1:(1/32):(6/32):30	12.3	20.8	3.5
6	1:(1/32):(8/32):30	8.1	13.7	2.3
7	1:(1/64):(6/64):30	7.8	13.4	2.2
8	1:(1/32):(6/32):50	9.9	27.5	4.6
9	1:(1/32):(6/32):80	7.5	32.6	5.5

<sup>[a]</sup> Graft content was calculated by <sup>1</sup>H NMR according to the literature [57]. <sup>[b]</sup> Graft length equaled graft content divided by 6%. <sup>[c]</sup> Polymerization was conducted without UV.

Controlled experiments in the absence of light source or any reagent were conducted. P(VDF-*co*-CTFE) with no PAN graft chains was obtained by the removal of UV irradiation (Table 1, run 1). To further illustrate the light-responsive nature of the polymerization, a series of polymerizations were tested by introducing an “off-on” sequence ([Cl]:[Cu]:[L]:[AN] = 1:(1/32):(6/32):30). In Figure 1, the graft content reached 2.1 mol % after 30 min and stayed almost unchanged during 30 min dark. The re-exposure to UV enabled the polymerization to start again. These cycles were repeated several times. The omission of P(VDF-*co*-CTFE) afforded no product (Table 1, run 2), which indicated that autopolymerization of AN did not occur under the current condition. In the absence of catalyst/ligand,

no graft content was observed (Table 1, run 3), which elucidated the control of activation/deactivation equilibrium by  $\text{CuCl}_2/\text{Me}_6\text{-Tren}$ .

The influence of  $[\text{Cu}]:[\text{L}]$  on graft polymerization was investigated. It was supposed that 1:6 would be better to yield a higher graft content (Table 1, runs 4, 5, and 6), which was consistent with previous reports [25,26]. Kinetics study showed a linear dependence between  $-\ln(1-\text{conversion})$  and reaction time. This confirmed that the polymerization rate was first-order with respect to the monomer concentration (Figure 2). Under the optimized reaction conditions, polymerizations with different monomer feed ratio were carried out to fabricate  $\text{P}(\text{VDF-co-CTFE})\text{-g-PAN}$  with varied graft contents (Table 1, runs 8 and 9). A chain extension experiment was conducted. The resultant  $\text{P}(\text{VDF-co-CTFE})\text{-g-PAN}$  (graft content = 20.8 mol %) was used as macroinitiator to initiate polymerization of AN ( $[\text{Cl}]:[\text{Cu}]:[\text{L}]:[\text{AN}] = 1:(1/32):(6/32):30$ , UV ( $\lambda_{\text{max}} = 365 \text{ nm}$ )). The graft content was increased into 30.2 mol % upon another 6 h exposure.

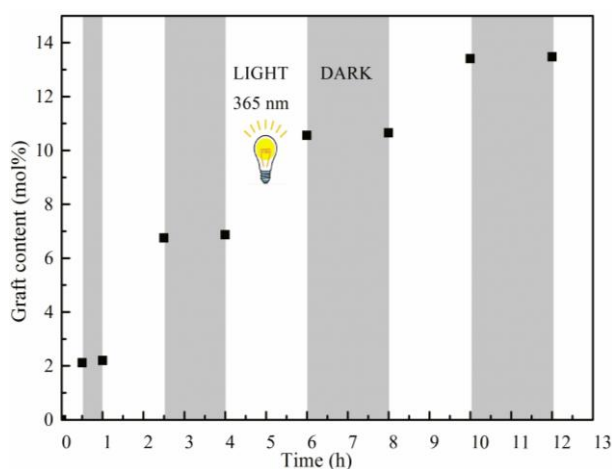


**Figure 1.** Graft contents vs. reaction time dependence for photoinduced  $\text{Cu}(\text{II})$ -mediated RDRP of AN in DMSO with  $\text{P}(\text{VDF-co-CTFE})$  as macroinitiator under “on-off” light sequence ( $[\text{Cl}]:[\text{Cu}]:[\text{L}]:[\text{AN}] = 1:(1/32):(6/32):30$ , UV ( $\lambda_{\text{max}} = 365 \text{ nm}$ )).

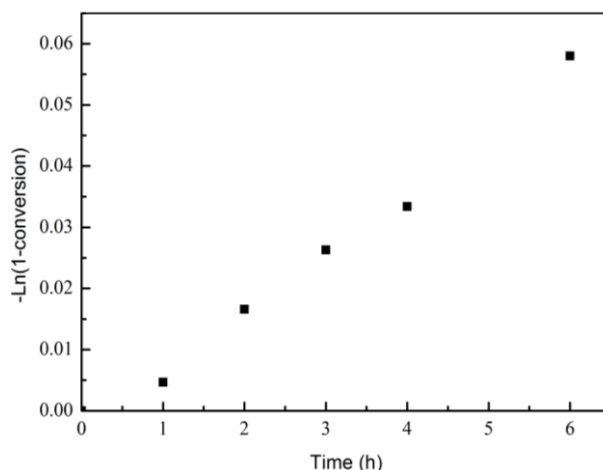


**Figure 2.** Semilogarithmic kinetic plots for photoinduced  $\text{Cu}(\text{II})$ -mediated RDRP of AN in DMSO with  $\text{P}(\text{VDF-co-CTFE})$  as macroinitiator ( $[\text{Cl}]:[\text{Cu}]:[\text{L}]:[\text{AN}] = 1:(1/32):(6/32):30$ , UV ( $\lambda_{\text{max}} = 365 \text{ nm}$ )).

The chemical structure of  $\text{P}(\text{VDF-co-CTFE})\text{-g-PAN}$  was characterized by FTIR,  $^1\text{H}$  NMR, and  $^{19}\text{F}$  NMR. In Figure 3, the characteristic absorption peak at  $2247 \text{ cm}^{-1}$  ( $-\text{CN}$ ) indicated the presence of PAN segments in the copolymer. The  $^1\text{H}$  NMR spectrum (Figure 4) displayed two multiple peaks of

head-head and head-tail connections of VDF units (2.2–2.4 ppm and 2.7–3.2 ppm). The shoulder peak at 3.0–3.3 ppm corresponded to the proton signal of VDF adjacent to CTFE ( $-\text{CF}_2\text{CH}_2\text{CFCICF}_2-$ ). A new peak appearing around 1.9–2.1 ppm was attributed to the proton on the methylene group of the AN unit ( $-\text{CH}_2\text{CHCN}-$ ). Another new peak appeared at 3.0–3.3 ppm and overlapped with the proton signals of head-to-tail connections of VDF in  $\text{P}(\text{VDF-}co\text{-CTFE})$ , which was assigned to the methine proton ( $-\text{CH}_2\text{CHCN}-$ ). The signals of  $-\text{CH}_2\text{CHF}_2-$  from hydrogenation of CTFE units and  $-\text{CH}=\text{CFICF}_2-$  from elimination of HCl from main chains were not observed. This indicated that the typical side reactions did not happen in this photoinduced Cu(II)-mediated RDRP process. The  $^{19}\text{F}$  NMR spectrum provided more information about the structure of graft copolymers. In Figure 5, the new peak appearing at 112.3 ppm was attributed to the AN units inserting into the C–Cl bond, where the C–C bond took the place of the C–Cl bond, which was consistent with the previous report [57]. No other new peaks were observed, which illustrated that the typical side reactions in traditional ATRP were avoided in this process.

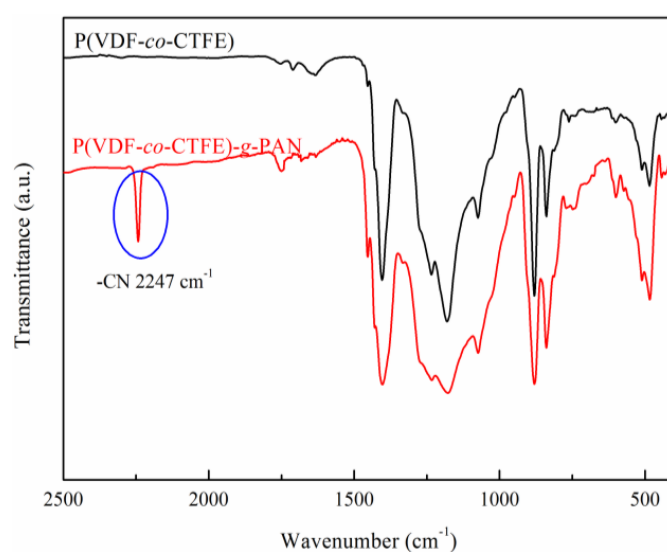


**Figure 3.** Fourier transform infrared (FTIR) spectrum of pristine  $\text{P}(\text{VDF-}co\text{-CTFE})$  and  $\text{P}(\text{VDF-}co\text{-CTFE})$ - $g$ -PAN (Table 1, run 5).

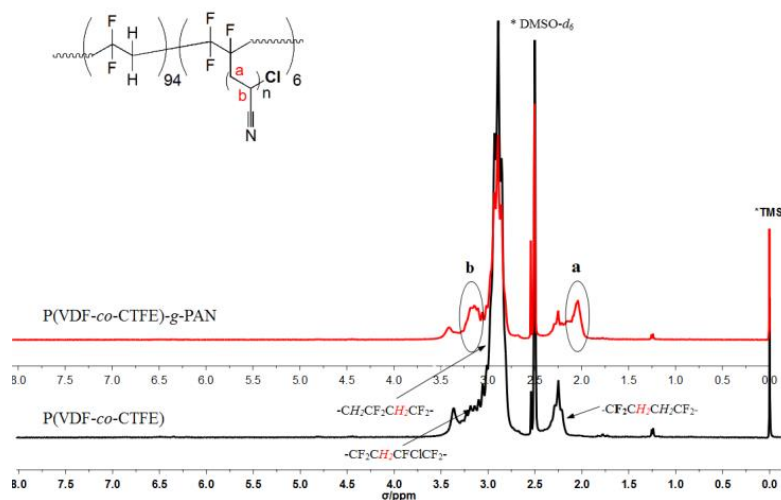


**Figure 4.**  $^1\text{H}$  NMR of pristine  $\text{P}(\text{VDF-}co\text{-CTFE})$  and  $\text{P}(\text{VDF-}co\text{-CTFE})$ - $g$ -PAN (Table 1, run 5).

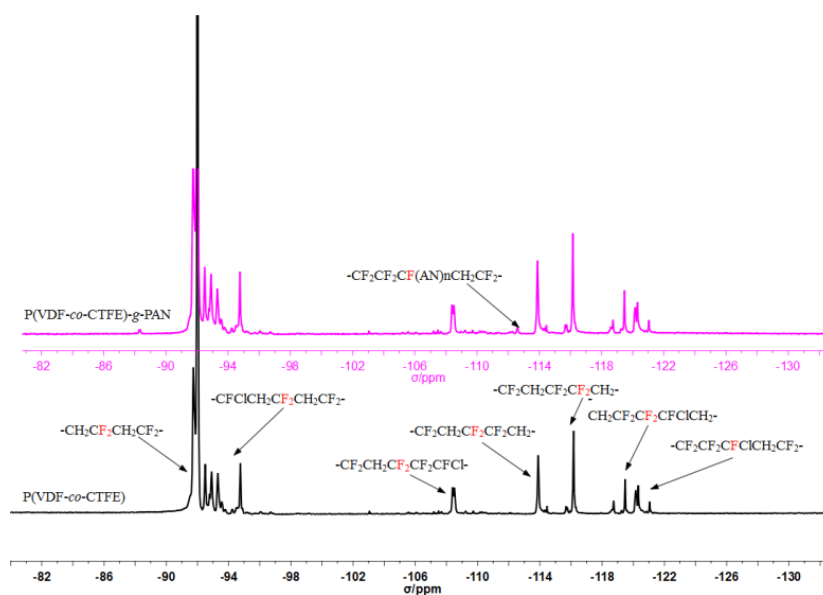


**Figure 5.**  $^{19}\text{F}$  NMR of pristine P(VDF-*co*-CTFE) and P(VDF-*co*-CTFE)-*g*-PAN (Table 1, run 5).

The thermal properties of P(VDF-*co*-CTFE)-*g*-PAN was explored by using DSC and TGA. In Figure 6, one endothermic peak was observed on each curve below 180 °C, which was assigned to the melting of the crystalline fluoropolymers. The melting temperature decreased from 149 to 137 °C with the increase of PAN graft content. This suggested that the crystalline degree of P(VDF-*co*-CTFE) and the crystal domain size were influenced by the introduction of PAN graft segments. The TGA (Figure 7) showed that the pristine P(VDF-*co*-CTFE) began to decompose at about 400 °C, and about 40 wt % remained at 500 °C. Meanwhile, two polymer degradation stages were observed for the P(VDF-*co*-CTFE)-*g*-PAN copolymers. The first stage started from about 300 °C, which corresponded to the decomposition of PAN segment. The second stage began from about 450 °C, which was attributed to the degradation of P(VDF-*co*-CTFE) backbone chain. It was noteworthy that the weight remaining over 500 °C was enhanced with the increase of PAN content. It was supposed that the PAN was carbonized to carbon material with higher thermal stability.

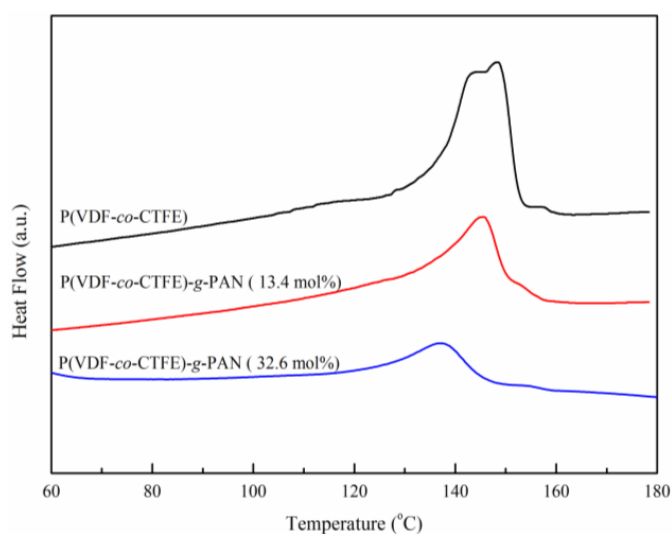


**Figure 6.** Differential scanning calorimetry (DSC) curves of pristine P(VDF-*co*-CTFE) and P(VDF-*co*-CTFE)-*g*-PAN with varied graft contents (Table 1, runs 7 and 9).

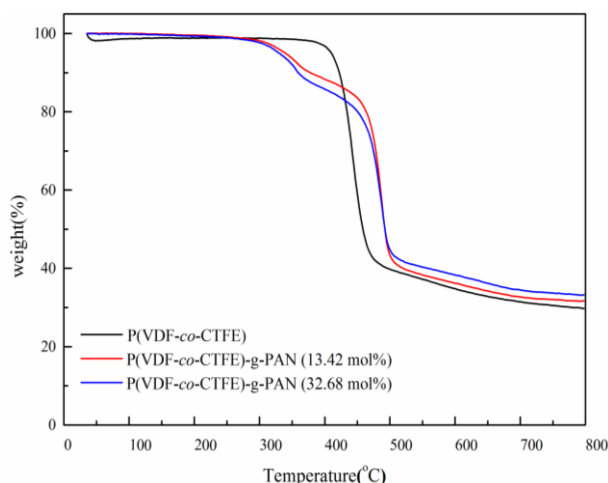


**Figure 7.** Thermogravimetric analysis (TGA) curves of pristine P(VDF-*co*-CTFE) and P(VDF-*co*-CTFE)-*g*-PAN copolymers with varied graft contents (Table 1, runs 7 and 9).

#### 4. Conclusions

In summary, poly(vinylidene fluoride-*co*-chlorotrifluoroethylene)-*graft*-polyacrylonitrile (P(VDF-*co*-CTFE)-*g*-PAN) with varied graft contents were prepared via photoinduced Cu(II)-mediated reversible deactivation radical polymerization (RDRP). Upon UV irradiation, CuCl<sub>2</sub>/Me<sub>6</sub>-Tren enabled low catalyst loading and temporal control of the polymerization process. This protocol might have potential application in the area of novel dielectric materials.

**Acknowledgments:** This work was supported by the National Natural Science Foundation of China (21604037 and 21522604).

**Author Contributions:** Xin Hu and Kai Guo conceived and designed the experiments; Xin Hu and Guopeng Cui performed the experiments; Xin Hu, Ning Zhu and Kai Guo analyzed the data; Ning Zhu and Jinglin Zhai contributed reagents/materials/analysis tools; Xin Hu wrote the paper.

**Conflicts of Interest:** The authors declare no conflict of interest.

#### References

1. Wang, J.; Matyjaszewski, K. Atom transfer radical polymerization in the presence of transition-metal complexes. *J. Am. Chem. Soc.* **1995**, *117*, 5614–5615. [[CrossRef](#)]
2. Kato, M.; Kamigaito, M.; Sawamoto, M.; Higashimura, T. Polymerization of Methyl Methacrylate with the Carbon Tetrachloride/Dichlorotris-(triphenylphosphine)ruthenium(II)/Methylaluminum Bis(2,6-di-*tert*-butylphenoxide) Initiating System: Possibility of Living Radical Polymerization. *Macromolecules* **1995**, *28*, 1721–1723. [[CrossRef](#)]
3. Matyjaszewski, K.; Xia, J. Atom Transfer Radical Polymerization. *Chem. Rev.* **2001**, *101*, 2921–2990. [[CrossRef](#)] [[PubMed](#)]
4. Matyjaszewski, K. Atom Transfer Radical Polymerization (ATRP): Current Status and Future Perspectives. *Macromolecules* **2012**, *45*, 4015–4039. [[CrossRef](#)]
5. Chiefari, J.; Chong, Y.; Ercole, F.; Krstina, J.; Jeffery, J.; Le, T.P.; Mayadunne, R.T.; Meijs, G.F.; Moad, C.L.; Moad, G. Living Free-Radical Polymerization by Reversible Addition-Fragmentation Chain Transfer: The RAFT Process. *Macromolecules* **1998**, *31*, 5559–5562. [[CrossRef](#)]
6. Boyer, C.; Bulmus, V.; Davis, T.P.; Ladmiral, V.; Liu, J.; Perrier, S. Bioapplications of RAFT Polymerization. *Chem. Rev.* **2009**, *109*, 5402–5436. [[CrossRef](#)] [[PubMed](#)]
7. Benot, D.; Chaplinski, V.; Raslau, R.B.; Hawker, C.J. Development of a Universal Alkoxyamine for “Living” Free Radical Polymerizations. *J. Am. Chem. Soc.* **1999**, *121*, 3904–3920. [[CrossRef](#)]
8. Hawker, C.J.; Bosman, A.W.; Harth, E. New Polymer Synthesis by Nitroxide Mediated Living Radical Polymerizations. *Chem. Rev.* **2001**, *101*, 3661–3688. [[CrossRef](#)] [[PubMed](#)]

9. Min, K.; Gao, H.; Matyjaszewski, K. Use of Ascorbic Acid as Reducing Agent for Synthesis of Well-Defined Polymers by ARGET ATRP. *Macromolecules* **2007**, *40*, 1789–1791. [[CrossRef](#)]
10. Matyjaszewski, K.; Jakubowski, W.; Min, K.; Tang, W.; Huang, J.Y.; Braunecker, W.A.; Tsarevsky, N.V. Diminishing catalyst concentration in atom transfer radical polymerization with reducing agents. *Proc. Natl. Acad. Sci. USA* **2006**, *103*, 15309–15314. [[CrossRef](#)] [[PubMed](#)]
11. Magenau, A.J.D.; Strandwitz, N.C.; Gennaro, A.; Matyjaszewski, K. Electrochemically Mediated Atom Transfer Radical Polymerization. *Science* **2011**, *332*, 81–84. [[CrossRef](#)] [[PubMed](#)]
12. Zhang, Y.; Wang, Y.; Matyjaszewski, K. ATRP of Methyl Acrylate with Metallic Zinc, Magnesium, and Iron as Reducing Agents and Supplemental Activators. *Macromolecules* **2011**, *44*, 683–685. [[CrossRef](#)]
13. Percec, V.; Guliashvili, T.; Ladislav, J.S.; Wistrand, A.; Stjern Dahl, A.; Sienkowska, M.J.; Monteiro, M.J.; Sahoo, S. Ultrafast Synthesis of Ultrahigh Molar Mass Polymers by Metal-Catalyzed Living Radical Polymerization of Acrylates, Methacrylates, and Vinyl Chloride Mediated by SET at 25 °C. *J. Am. Chem. Soc.* **2006**, *128*, 14156–14165. [[CrossRef](#)] [[PubMed](#)]
14. Anastasaki, A.; Nikolaou, V.; Nurumbetov, G.; Wilson, P.; Kempe, K.; Quinn, J.F.; Davis, T.P.; Whittaker, M.R.; Haddleton, D.M. Cu(0)-Mediated Living Radical Polymerization: A Versatile Tool for Materials Synthesis. *Chem. Rev.* **2016**, *116*, 835–877. [[CrossRef](#)] [[PubMed](#)]
15. Anastasaki, A.; Nikolaou, V.; Haddleton, D.M. Cu(0)-mediated living radical polymerization: recent highlights and applications; a perspective. *Polym. Chem.* **2016**, *7*, 1002–1026. [[CrossRef](#)]
16. Shanmugam, S.; Boyer, C. Organic photocatalysts for cleaner polymer synthesis. *Science* **2016**, *352*, 1053–1054. [[CrossRef](#)] [[PubMed](#)]
17. Dadashi-Silab, S.; Doran, S.; Yagci, Y. Photoinduced Electron Transfer Reactions for Macromolecular Syntheses. *Chem. Rev.* **2016**, *116*, 10212–10275. [[CrossRef](#)] [[PubMed](#)]
18. Chen, M.; Zhong, M.; Johnson, J.A. Light-Controlled Radical Polymerization: Mechanisms, Methods, and Applications. *Chem. Rev.* **2016**, *116*, 10167–10211. [[CrossRef](#)] [[PubMed](#)]
19. Zivic, N.; Bouzrati-Zerelli, M.; Kermagoret, A.; Dumur, F.; Fouassier, J.; Gigmes, D.; Lalevé, J. Photocatalysts in Polymerization Reactions. *Chem. Cat. Chem.* **2016**, *8*, 1617–1631. [[CrossRef](#)]
20. Pan, X.; Tasdelen, M.A.; Laun, J.; Junkers, T.; Yagci, Y.; Matyjaszewski, K. Photomediated controlled radical polymerization. *Prog. Polym. Sci.* **2016**, *62*, 73–125. [[CrossRef](#)]
21. Tasdelen, M.A.; Uygun, M.; Yagci, Y. Photoinduced Controlled Radical Polymerization in Methanol. *Macromol. Chem. Phys.* **2010**, *211*, 2271–2275. [[CrossRef](#)]
22. Tasdelen, M.A.; Uygun, M.; Yagci, Y. Photoinduced Controlled Radical Polymerization. *Macromol. Rapid Commun.* **2011**, *32*, 58–62. [[CrossRef](#)] [[PubMed](#)]
23. Konkolewicz, D.; Schroder, K.; Buback, J.; Bernhard, S.; Matyjaszewski, K. Visible Light and Sunlight Photoinduced ATRP with ppm of Cu Catalyst. *ACS Macro Lett.* **2012**, *1*, 1219–1223. [[CrossRef](#)]
24. Ribelli, T.G.; Konkolewicz, D.; Bernhard, S.; Matyjaszewski, K. How are Radicals (Re)Generated in Photochemical ATRP? *J. Am. Chem. Soc.* **2014**, *136*, 13303–13312. [[CrossRef](#)] [[PubMed](#)]
25. Anastasaki, A.; Nikolaou, V.; Zhang, Q.; Burns, J.; Samanta, S.R.; Wladron, C.; Haddleton, A.J.; McHale, R.; Fox, D.; Percec, V.; et al. Copper(II)/Tertiary Amine Synergy in Photoinduced Living Radical Polymerization: Accelerated Synthesis of  $\omega$ -Functional and  $\alpha,\omega$ -Heterofunctional Poly(acrylates). *J. Am. Chem. Soc.* **2014**, *136*, 1141–1149. [[CrossRef](#)] [[PubMed](#)]
26. Jones, G.R.; Whitfield, R.; Anastasaki, A.; Haddleton, D.M. Aqueous Copper(II) Photoinduced Polymerization of Acrylates: Low Copper Concentration and the Importance of Sodium Halide Salts. *J. Am. Chem. Soc.* **2016**, *138*, 7346–7352. [[CrossRef](#)] [[PubMed](#)]
27. Anastasaki, A.; Nkkolaou, V.; McCaul, N.W.; Simular, A.; Godfrey, J.; Waldron, C.; Wilson, P.; Kempe, K.; Haddleton, D.M. Photoinduced Synthesis of  $\alpha,\omega$ -Telechelic Sequence-Controlled Multiblock Copolymers. *Macromolecules* **2015**, *48*, 1404–1411. [[CrossRef](#)]
28. Anastasaki, A.; Nikolaou, V.; Simular, A.; Godfrey, J.; Li, M.; Nurumbetov, G.; Wilson, P.; Haddleton, D.M. Expanding the Scope of the Photoinduced Living Radical Polymerization of Acrylates in the Presence of CuBr<sub>2</sub> and Me<sub>6</sub>-Tren. *Macromolecules* **2014**, *47*, 3852–3859. [[CrossRef](#)]
29. Anastasaki, A.; Nikolaou, V.; Pappas, G.S.; Zhang, Q.; Wan, C.Y.; Wilson, P.; Davis, T.P.; Whittaker, M.R.; Haddleton, D.M. Photoinduced sequence-control via one pot living radical polymerization of acrylates. *Chem. Sci.* **2014**, *5*, 3536–3542. [[CrossRef](#)]

30. Chuang, Y.M.; Ethirajan, A.; Junkers, T. Photoinduced Sequence-Controlled Copper-Mediated Polymerization: Synthesis of Decablock Copolymers. *ACS Macro Lett.* **2014**, *3*, 732–737. [[CrossRef](#)]
31. Chuang, Y.M.; Wenn, B.; Gielen, S.; Ethirajan, A.; Junkers, T. Ligand switch in photoinduced copper-mediated polymerization: synthesis of methacrylate-acrylate block copolymers. *Polym. Chem.* **2015**, *6*, 6488–6497. [[CrossRef](#)]
32. Vandenberg, J.; Reekmans, G.; Adriaensens, P.; Junkers, T. Synthesis of sequence-defined acrylate oligomers via photo-induced copper-mediated radical monomer insertions. *Chem. Sci.* **2015**, *6*, 5753–5761. [[CrossRef](#)]
33. Frick, E.; Anastasaki, A.; Haddleton, D.M.; Barner-Kowollik, C. Enlightening the Mechanism of Copper Mediated PhotoRDRP via High-Resolution Mass Spectrometry. *J. Am. Chem. Soc.* **2015**, *137*, 6889–6896. [[CrossRef](#)] [[PubMed](#)]
34. Discekici, E.H.; Anastasaki, A.; Kaminker, R.; Willenbacher, J.; Truong, N.P.; Fleischmann, C.; Oschmann, B.; Lunn, D.J.; de Alaniz, J.R.; Davis, T.P.; et al. Light-Mediated Atom Transfer Radical Polymerization of Semi-Fluorinated (Meth)acrylates: Facile Access to Functional Materials. *J. Am. Chem. Soc.* **2017**, *139*, 5939–5945. [[CrossRef](#)] [[PubMed](#)]
35. Laun, J.; Vorobii, M.; Pereira, A.D.; Pop-Georgievski, O.; Trouillet, V.; Welle, A.; Barner-Kowollik, C.; Rodriguez-Emmenegger, C.; Junkers, T. Surface Grafting via Photo-Induced Copper-Mediated Radical Polymerization at Extremely Low Catalyst Concentrations. *Macromol. Rapid Commun.* **2015**, *36*, 1681–1686. [[CrossRef](#)] [[PubMed](#)]
36. Fors, B.P.; Hawker, C.J. Control of a Living Radical Polymerization of Methacrylates by Light. *Angew. Chem. Int. Ed.* **2012**, *51*, 8850–8853. [[CrossRef](#)] [[PubMed](#)]
37. Treat, N.J.; Fors, B.P.; Kramer, J.W.; Christianson, M.; Chiu, C.; Alaniz, J.R.; Hawker, C.J. Controlled Radical Polymerization of Acrylates Regulated by Visible Light. *ACS Macro Lett.* **2014**, *3*, 580–584. [[CrossRef](#)]
38. Poelma, J.E.; Fors, B.P.; Meyers, G.F.; Kramer, J.W.; Hawker, C.J. Fabrication of Complex Three-Dimensional Polymer Brush Nanostructures through Light-Mediated Living Radical Polymerization. *Angew. Chem. Int. Ed.* **2013**, *52*, 6844–6848. [[CrossRef](#)] [[PubMed](#)]
39. Melker, A.; Fors, B.P.; Hawker, C.J.; Poelma, E.J. Continuous flow synthesis of poly(methyl methacrylate) via a light-mediated controlled radical polymerization. *J. Polym. Sci. A* **2015**, *53*, 2693–2698. [[CrossRef](#)]
40. Zhang, G.; Song, I.Y.; Ahn, K.H.; Park, T.; Choi, W. Free Radical Polymerization Initiated and Controlled by Visible Light Photocatalysis at Ambient Temperature. *Macromolecules* **2011**, *44*, 7594–7599. [[CrossRef](#)]
41. Treat, T.J.; Sprafke, H.; Kramer, J.W.; Clark, P.G.; Barton, B.E.; de Alaniz, J.R.; Fors, B.P.; Hawker, C.J. Metal-Free Atom Transfer Radical Polymerization. *J. Am. Chem. Soc.* **2014**, *136*, 16096–16101. [[CrossRef](#)] [[PubMed](#)]
42. Miyake, G.M.; Theriot, J.C. Perylene as an Organic Photocatalyst for the Radical Polymerization of Functionalized Vinyl Monomers through Oxidative Quenching with Alkyl Bromides and Visible Light. *Macromolecules* **2014**, *47*, 8255–8261. [[CrossRef](#)]
43. Pan, X.; Lamson, M.; Yan, J.; Matyjaszewski, K. Photoinduced Metal-Free Atom Transfer Radical Polymerization of Acrylonitrile. *ACS Macro Lett.* **2015**, *4*, 192–196. [[CrossRef](#)]
44. Pan, X.; Fang, C.; Fantin, M.; Malhotra, N.; So, W.Y.; Peteanu, L.A.; Isse, A.A.; Gennaro, A.; Liu, P.; Matyjaszewski, K. Mechanism of Photoinduced Metal-Free Atom Transfer Radical Polymerization: Experimental and Computational Studies. *J. Am. Chem. Soc.* **2016**, *138*, 2411–2452. [[CrossRef](#)] [[PubMed](#)]
45. Liu, X.; Zhang, L.; Cheng, Z.; Zhu, X. Metal-free photoinduced electron transfer-atom transfer radical polymerization (PET-ATRP) via a visible light organic photocatalyst. *Polym. Chem.* **2016**, *7*, 689–700. [[CrossRef](#)]
46. Theriot, J.C.; Lim, C.; Yang, H.; Ryan, M.D.; Musgrave, C.B.; Miyake, G.M. Organocatalyzed atom transfer radical polymerization driven by visible light. *Science* **2016**, *352*, 1082–1086. [[CrossRef](#)] [[PubMed](#)]
47. Pearson, R.M.; Lim, C.; McCarthy, B.G.; Musgrave, C.B.; Miyake, G.M. Organocatalyzed Atom Transfer Radical Polymerization Using *N*-Aryl Phenoxazines as Photoredox Catalysts. *J. Am. Chem. Soc.* **2016**, *138*, 11399–11407. [[CrossRef](#)] [[PubMed](#)]
48. Lim, C.; Ryan, M.D.; McCarthy, B.G.; Theriot, J.C.; Sartor, S.M.; Damrauer, N.H.; Musgrave, C.B.; Miyake, G.M. Intramolecular Charge Transfer and Ion Pairing in *N,N*-Diaryl Dihydrophenazine Photoredox Catalysts for Efficient Organocatalyzed Atom Transfer Radical Polymerization. *J. Am. Chem. Soc.* **2017**, *139*, 348–355. [[CrossRef](#)] [[PubMed](#)]

49. Dadashi-Silab, S.; Pan, X.; Matyjaszewski, K. Phenyl Benzo[b]phenothiazine as a Visible Light Photoredox Catalyst for Metal-Free Atom Transfer Radical Polymerization. *Chem. Eur. J.* **2017**, *23*, 5972–5977. [[CrossRef](#)] [[PubMed](#)]
50. Ryan, M.D.; Pearson, R.M.; French, T.A.; Miyake, G.M. Impact of Light Intensity on Control in Photoinduced Organocatalyzed Atom Transfer Radical Polymerization. *Macromolecules* **2017**, *50*, 4616–4622. [[CrossRef](#)]
51. Ramsey, B.L.; Pearson, R.M.; Beck, L.R.; Miyake, G.M. Photoinduced Organocatalyzed Atom Transfer Radical Polymerization Using Continuous Flow. *Macromolecules* **2017**, *50*, 2668–2674. [[CrossRef](#)] [[PubMed](#)]
52. Chu, B.; Zhan, X.; Ren, K.; Neese, B.; Lin, M.; Wang, Q.; Bauer, F.; Zhang, Q. A Dielectric Polymer with High Electric Energy Density and Fast Discharge Speed. *Science* **2006**, *313*, 334–336. [[CrossRef](#)] [[PubMed](#)]
53. Guan, F.; Pan, J.; Wang, J.; Wang, Q.; Zhu, L. Crystal Orientation Effect on Electric Energy Storage in Poly(vinylidene fluoride-co-hexafluoropropylene) Copolymers. *Macromolecules* **2010**, *43*, 384–392. [[CrossRef](#)]
54. Li, J.; Hu, X.; Gao, G.; Ding, S.; Li, H.; Yang, L.; Zhang, Z. Tuning phase transition and ferroelectric properties of poly(vinylidene fluoride-co-trifluoroethylene) via grafting with desired poly(methacrylic ester)s as side chains. *J. Mater. Chem. C* **2013**, *1*, 1111–1121. [[CrossRef](#)]
55. Li, J.; Tan, S.; Ding, S.; Li, H.; Yang, L.; Zhang, Z. High-field antiferroelectric behaviour and minimized energy loss in poly(vinylidene-co-trifluoroethylene)-graft-poly(ethyl methacrylate) for energy storage application. *J. Mater. Chem.* **2012**, *22*, 23468–23476. [[CrossRef](#)]
56. Tan, S.; Liu, E.; Zhang, Q.; Zhang, Z. Controlled hydrogenation of P(VDF-co-CTFE) to prepare P(VDF-co-TrFE-co-CTFE) in the presence of CuX (X = Cl, Br) complexes. *Chem. Commun.* **2011**, *47*, 4544–4546. [[CrossRef](#)] [[PubMed](#)]
57. Hu, X.; Li, J.; Li, H.; Zhang, Z. Synthesis and characterization of poly(vinylidene fluoride-co-chlorotrifluoroethylene)-grafted-poly(acrylonitrile) via single electron transfer-living radical polymerization process. *J. Polym. Sci. A* **2012**, *50*, 3126–3134. [[CrossRef](#)]
58. Hu, X.; Li, J.; Li, H.; Zhang, Z. Cu(0)/2,6-bis(imino)pyridines catalyzed single-electron transfer-living radical polymerization of methyl methacrylate initiated with poly(vinylidene fluoride-co-chlorotrifluoroethylene). *J. Polym. Sci. A* **2013**, *51*, 4378–4388. [[CrossRef](#)]
59. Hu, X.; Tan, S.; Gao, G.; Xie, Y.; Wang, Q.; Li, N.; Zhang, Z. Synthesis of unsaturation containing P(VDF-co-TrFE-co-CTFE) from P(VDF-co-CTFE) in one-pot catalyzed with Cu(0)-based single electron transfer living radical polymerization system. *J. Polym. Sci. A* **2014**, *52*, 3429–3440. [[CrossRef](#)]
60. Zhu, N.; Hu, X.; Zhang, Y.; Zhang, K.; Li, Z.; Guo, K. Continuous flow SET-LRP in the presence of P(VDF-co-CTFE) as macroinitiator in a copper tubular reactor. *Polym. Chem.* **2016**, *7*, 474–480. [[CrossRef](#)]



© 2018 by the authors. Licensee MDPI, Basel, Switzerland. This article is an open access article distributed under the terms and conditions of the Creative Commons Attribution (CC BY) license (<http://creativecommons.org/licenses/by/4.0/>).